Inorganic Chemistry
Article

Inorg. Chem. **2010**, *49*, 6897–6903 **6897**
DOI: 10.1021/ic1004177

Synthesis and Properties of Dinuclear Ru(II)/Os(II) Complexes Based on a Heteroditopic Phenanthroline−Terpyridine Bridging Ligand

Eugenio Coronado,[†] Pablo Gaviña,*[,†] Sergio Tatay,[†] Robert Groarke,[‡] and Johannes G. Vos*[,‡]

[†]*Instituto de Ciencia Molecular, Universidad de Valencia, 46980 Paterna (Valencia), Spain, and*
[‡]*Solar Energy Conversion SRC, School of Chemical Sciences, Dublin City University, Dublin 9, Ireland*

Received March 2, 2010

The synthesis and characterization of a series of mono- and dinuclear ruthenium(II) and osmium(II) polypyridyl complexes based on the heteroditopic bridging ligand **PT** are reported. This ligand incorporates bidentate phen (1,10-phenanthroline) and terdentate tpy (2,2′:6′,2″-terpyridine) units directly connected by their 3 and 5 positions, respectively. The dinuclear complexes have been synthesized via a Pd(0) catalyzed cross-coupling reaction between a bromo-substituted Ru−phen complex and a tpy derivative incorporating a boronate ester, followed by Ru(II) or Os(II) complexation. The compounds obtained are fully characterized using spectroscopic and electrochemical measurements. The electrochemical studies do not yield any evidence for interaction between the two metal centers in the dinuclear compounds. Emission studies indicate, however, energy transfer from the phen moiety to the tpy center. For the ruthenium/osmium species, this process is relatively slow, resulting in a dual emission. The emission of the mononuclear ruthenium compound is enhanced by the addition of Zn(II).

Introduction

Polypyridyl ruthenium(II) complexes based on 2,2′-bipyridine (bpy), 1,10-phenanthroline (phen), or 2,2′:6′,2″-terpyridine (tpy) ligands possess interesting photophysical, photochemical, and electrochemical characteristics[1−4] which make them appealing for the construction of luminescent sensors and photoactive molecular-scale devices.[5−11] The covalent linkage of various (polypyridine)metal complexes to generate multimetallic assemblies has further expanded these possibilities and has provided a unique framework for the fundamental study of intramolecular energy and electron transfer processes in the excited state.[12−15] Tris-bidentate moieties such as $[Ru(bpy)_3]^{2+}$ or $[Os(bpy)_3]^{2+}$ are ideal models for the construction of such assemblies, due to their excellent photophysical and photochemical properties compared to the bis-terdentate complexes. However, from a synthetic viewpoint, the use of bidentate ligands is less convenient, as they afford chiral tris-bidentate complexes leading to mixtures of diastereomers, which are often difficult to separate. In contrast, symmetric terdentate ligands, such as a tpy substituted at the 4′ position, have provided a convenient way to incorporate bis-terdentate complexes into linear achiral assemblies, and several $Ru(tpy)_2-M(tpy)_2$ (M = Ru(II), Os(II)) diads and triads have been reported.[16,18] However, rigidly linked dinuclear metal complexes, containing both bis-terdentate and tris-bidentate chromophores, have received less attention.[19−23]

*To whom correspondence should be addressed. Tel.: +34 963544421 (P.G.), +353 1 7005307 (J.G.V.). Fax: +34 963543273 (P.G.), +353 1 7005503(J.G.V.). E-mail: pablo.gavina@uv.es (P.G.), han.vos@dcu.ie (J.G.V.).

(1) Meyer, T. J. *Pure Appl. Chem.* **1986**, *58*, 1193–1206.
(2) Juris, A.; Balzani, V.; Barigelletti, F.; Campagna, S.; Belser, P.; von Zelewsky, A. *Coord. Chem. Rev.* **1988**, *84*, 85–277.
(3) Balzani, V.; Juris, A.; Venturi, M.; Campagna, S.; Serroni, S. *Chem. Rev.* **1996**, *96*, 759–834.
(4) Campagna, S.; Puntoriero, F.; Nastasi, F.; Bergamini, G.; Balzani, V. *Top. Curr. Chem.* **2007**, *280*, 117–214.
(5) Keefe, M. H.; Benkstein, K. D.; Hupp, J. T. *Coord. Chem. Rev.* **2000**, *205*, 201–228.
(6) Rau, S.; Buttner, T.; Temme, C.; Gorls, H.; Walther, D.; Duati, M.; Fanni, S.; Vos, J. G. *Inorg. Chem.* **2000**, *39*, 1621–1624.
(7) Bignozzi, C. A.; Argazzi, R.; Kleverlaan, C. J. *Chem. Soc. Rev.* **2000**, *29*, 87–96.
(8) Sun, L.; Hammarström, L.; Åkermark, B.; Styring, S. *Chem. Soc. Rev.* **2001**, *30*, 36–49.
(9) Vos, J. G.; Kelly, J. M. *Dalton Trans.* **2006**, 4869–4883.
(10) Rau, S.; Walther, D.; Vos, J. G. *Dalton Trans.* **2007**, 915–919.
(11) Bonnet, S.; Collin, J.-P. *Chem. Soc. Rev.* **2008**, *37*, 1207–1217.
(12) De Cola, L.; Belser, P. *Coord. Chem. Rev.* **1998**, *177*, 301–346.
(13) Barigelletti, F.; Flamigni, L. *Chem. Soc. Rev.* **2000**, *29*, 1–12.
(14) Welter, S.; Salluce, N.; Belser, P.; Groeneveld, M.; De Cola, L. *Coord. Chem. Rev.* **2005**, *249*, 1360–1371.
(15) Chiorboli, C.; Indelli, M.; Scandola, F. *Top. Curr. Chem.* **2005**, *257*, 63–102.
(16) Sauvage, J.-P.; Collin, J.-P.; Chambron, J. C.; Guillerez, S.; Coudret, C.; Balzani, V.; Barigelletti, F.; De Cola, L.; Flamigni, L. *Chem. Rev.* **1994**, *94*, 993–1019.
(17) Medlycott, E. A.; Hanan, G. S. *Coord. Chem. Rev.* **2006**, *250*, 1763–1782.
(18) Encinas, S.; Flamigni, L.; Barigelletti, F.; Constable, E. C.; Housecroft, C. E.; Schofield, E. R.; Figgemeier, E.; Fenske, D.; Neuberger, M.; Vos, J. G.; Zehnder, M. *Chem.—Eur. J.* **2002**, *8*, 137–150.
(19) Harriman, A.; Hissler, M.; Khatyr, A.; Ziessel, R. *Eur. J. Inorg. Chem.* **2003**, *2003*, 955–959.
(20) Harriman, A.; Khatyr, A.; Ziessel, R. *Dalton Trans.* **2003**, 2061–2068.
(21) Constable, E. C.; Figgemeier, E.; Housecroft, C. E.; Olsson, J.; Zimmermann, Y. C. *Dalton Trans.* **2004**, 1918–1927.
(22) Figgemeier, E.; Constable, E. C.; Housecroft, C. E.; Zimmermann, Y. C. *Langmuir* **2004**, *20*, 9242–9248.
(23) Arm, K. J.; Williams, J. A. G. *Dalton Trans.* **2006**, 2172–2174.

Published on Web 07/02/2010

Chart 1. Structures of Ligand **PT** and the Mono- and Dinuclear Complexes

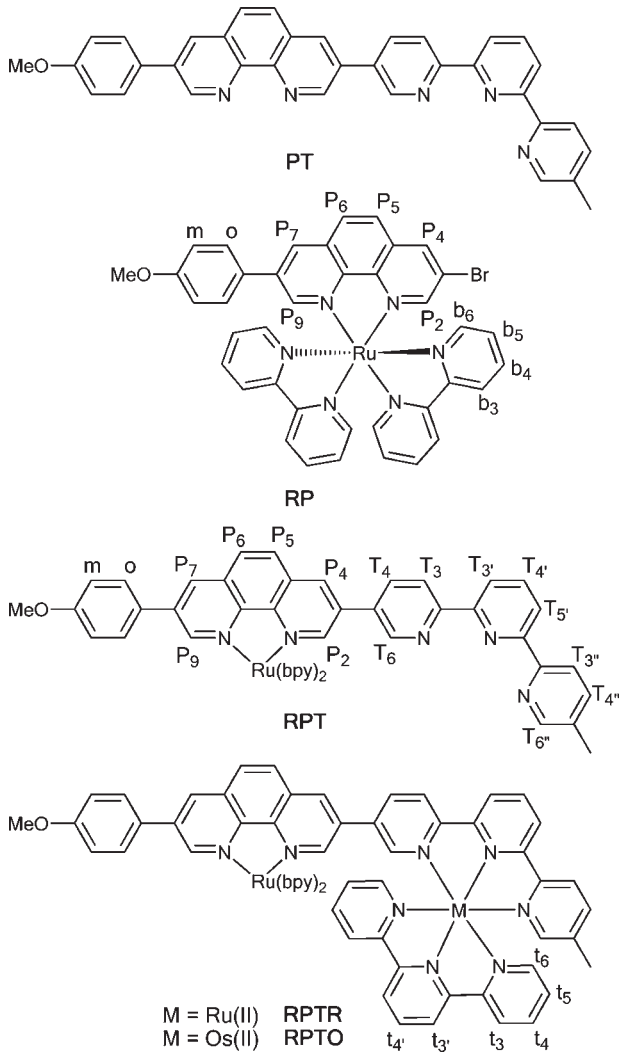

Recently, we described the synthesis of **PT** (Chart 1),[24,25] an azaaromatic heteroditopic ligand containing a phen bidentate unit and a tpy terdentate unit directly connected via the 3 and 5 positions, respectively. This ligand was used as a building block for the self-assembly of a metallosupramolecular hexamer based on Cu(II).[25] In this contribution, we present two new dinuclear Ru(II)−Ru(II) and Ru(II)−Os(II) complexes based on the use of **PT** as a bridging ligand. These complexes have been synthesized using stepwise cross-coupling and complexation reactions. In the first step, a bromophenanthroline Ru(II) tris-bidentate complex (**RP**) was reacted with a boronic ester tpy derivative in the presence of a catalytic amount of Pd(0) to yield the mononuclear Ru complex **RPT**, which was subsequently reacted with [Ru(tpy)Cl_3] or [Os(tpy)Cl_3] to give rise to the final Ru−Ru and Ru−Os dinuclear complexes **RPTR** and **RPTO** (Chart 1). The compounds obtained are fully characterized, and their electrochemical and electronic properties are discussed.

Experimental Section

Materials. All solvents used for absorption and emission spectroscopy were of spectroscopic grade (Sigma-Aldrich). All other reagents were of HPLC or analytic grade. *cis*-[Ru(bpy)$_2$$Cl_2$]·$2H_2O$ was purchased from Aldrich and used with no further purification. Ligands **1**, **2**, and **PT**[24,25] and complexes [Ru(tpy)Cl_3][26] and [Os(tpy)Cl_3][27] were prepared as previously reported. Thin-layer chromatography (TLC) was carried out on alumina sheets coated with silica gel 60 F_{254} (Merck). The TLC plates were eluted with acetonitrile/H_2O/sat. aq. KNO_3 (**RPT** and **RPTO**) or acetone/H_2O/sat. aq. KNO_3 (**RPTR**) and examined under a UV lamp. Prior to the photophysical studies, all of the complexes were recrystallized from isopropyl ether/CH_3CN by vapor diffusion.

[Ru(bpy)$_2$(1)][PF_6]$_2$ (RP). 3-Bromo-8-(p-anisyl)-1,10-phenanthroline (**1**) (0.37 g, 1.0 mmol), *cis*-[Ru(bpy)$_2$$Cl_2$]·$2H_2O$ (0.48 g, 1.0 mmol), and ethylene glycol (25 mL) were heated under Ar at 150 °C overnight. After cooling to room temperature, 50 mL of aqueous KPF_6 was added. The resulting precipitate was filtered under suction and used without further purification (orange solid; 0.99 g, 90%). ^{1}H NMR (CD_3CN, 300 MHz): 8.82 (d, J = 1.8 Hz, 1H, P_4), 8.77 (d, J = 1.8 Hz, 1H, P_7), 8.55−8.45 (m, 4H, $4b_3$), 8.28 (d, J = 8.9 Hz, 1H, P_5/P_6), 8.16 (d, J = 8.9 Hz, 1H, P_5/P_6), 8.14−7.97 (m, 6H, P_2, P_9, $4b_4$), 7.85−7.80 (m, 2H, $2b_6$), 7.65−7.60 (m, 2H, $2b_{6'}$), 7.52−7.42 (m, 4H, $2H_o$, $2b_5$), 7.28−7.20 (m, 2H, $2b_{5'}$), 7.03 (d, J = 8.9 Hz, 2H, $2H_m$), 3.83(s, 3H, CH_3O). HRMS(ES): m/z 923.03 ([M − PF_6]$^+$; calcd, 923.35), 389.05 ([M − 2PF_6]$^{2+}$; calcd, 389.30).

[Ru(bpy)$_2$(PT)][PF_6]$_2$ (RPT). A deaerated mixture of **RP** (1.1 g, 1.0 mmol), 5-neopentyl glycolatoboryl-5″-methyl-2,2′:6′,2″-terpyridine (**2**) (0.37 g, 1.0 mmol), Pd(PPh_3)$_4$ (0.092 g, 0.080 mmol), K_2CO_3 (0.69 g, 5.0 mmol), DMF (30 mL), and water (1.2 mL) was heated under Ar at 80 °C for 18 h. The mixture was cooled down to room temperature, and aqueous KPF_6 was added (150 mL). The resulting solid was filtered and purified by column chromatography on silica gel (eluent CH_2Cl_2/MeOH, gradient elution from 99:1 to 90:10) to obtain the desired product as an orange solid (0.62 g, 50% yield). ^{1}H NMR (CD_3CN, 300 MHz): δ 8.97 (d, J = 1.8 Hz, 1H, P_4), 8.86 (d, J = 2.0 Hz, 1H, T_6), 8.81 (d, J = 1.8 Hz, 1H, P_7), 8.77 (d, J = 8.3 Hz, 1H, T_3), 8.59−8.42 (m, 8H, $4b_3$, $T_{3'}$, $T_{5'}$, $T_{3''}$, $T_{6''}$), 8.31 (s, 2H, P_5, P_6), 8.27 (d, J = 1.8 Hz, 1H, P_2), 8.16−7.97 (m, 7H, $4b_4$, P_9, T_4, $T_{4'}$), 7.91 (bt, J = 5.2 Hz, 2H, $2b_6$), 7.79 (dd, J = 8.3 and 1.5 Hz, 1H, $T_{4''}$), 7.75 (d, J = 5.7 Hz, 1H, $b_{6'}$), 7.71 (d, J = 5.1 Hz, 1H, $b_{6'}$), 7.52 (d, J = 8.8 Hz, 2H, $2H_o$), 7.50−7.45 (m, 2H, $2b_5$), 7.29−7.24 (m, 2H, $2b_{5'}$), 7.04 (d, J = 8.8 Hz, 2H, $2H_m$), 3.84 (s, 3H, CH_3O), 2.42 (s, 3H, CH_3). HRMS(ES): m/z 1090.08 ([M − PF_6]$^+$; calcd, 1090.22), 473.65 ([M + H − 2PF_6]$^{2+}$; calcd, 473.63), 315.70 ([M + H − 2PF_6]$^{3+}$; calcd, 316,09). TLC, R_f = 0.2 in MeCN/H_2O/aq. KNO_3 = 9:1:0.3.

[Ru(bpy)$_2$(PT)Ru(tpy)][PF_6]$_4$ (RPTR). A solution of **RPT** (0.37 g, 0.30 mmol) and [Ru(tpy)Cl_3] (0.13 g, 0.30 mmol) in ethylene glycol (8 mL) was heated under Ar at 150 °C overnight. The mixture was cooled to room temperature, and aqueous KPF_6 was added (50 mL). The resulting precipitate was filtered and purified by column chromatography (silica gel, acetone/H_2O/sat. aq. KNO_3, 9:1:0.5 as eluent) followed by anion exchange with KPF_6 to yield **RPTR** as an orange-red powder (0.26 g, 47%). ^{1}H NMR (CD_3CN, 300 MHz): δ 8.79−8.66 (m, 5H, P_7, $2t_{3'}$, 2T), 8.56 (d, J = 8.4 Hz, 1H, $T_{3''}$), 8.53−8.38 (m, 9H, P_2, $4b_3$, $2t_3$, $t_{4'}$, $T_{4'}$), 8.36 (d, J = 8.0 Hz, 1H, 1T), 8.26 (d, J = 8.9 Hz, 1H, P_5/P_6), 8.15 (d, J = 8.9 Hz, 1H, P_5/P_6), 8.14−8.07 (m, 2H, $2b_4$), 8.06 (d, J = 1.8 Hz, 1H, P_9), 8.04−7.97 (m, 3H, $2b_4$, 1T), 7.95−7.90 (m, 3H, $2t_4$, T_6), 7.77 (dd, J = 5.6, 0.8 Hz, 1H, b_6), 7.72

(24) Gaviña, P.; Tatay, S. *Tetrahedron Lett*. **2006**, *47*, 3471–3473.
(25) Coronado, E.; Galan-Mascaros, J. R.; Gaviña, P.; Martí-Gastaldo, C.; Romero, F. M.; Tatay, S. *Inorg. Chem*. **2008**, *47*, 5197–5203.
(26) Sullivan, B. P.; Calvert, J. M.; Meyer, T. J. *Inorg. Chem*. **1980**, *19*, 1404–1407.
(27) Buckingham, D.; Dwyer, F.; Sargeson, A. *Aust. J. Chem*. **1964**, *17*, 622–631.

(dd, J = 8.0 and 1.7 Hz, 1H, 1T), 7.67 (dd, J= 5.6, 0.7 Hz, 1H, b_6), 7.56−7.50 (m, 2H, $2b_6$), 7.48 (d, J = 8.9 Hz, 2H, $2H_o$), 7.46−7.39 (m, 2H, $2b_5$), 7.37−7.31 (m, 3H, $2t_6$, $T_{6''}$), 7.25−7.19 (m, 2H, $2b_5$), 7.20−7.09 (m, 2H, $2t_5$), 7.02 (d, J = 8.9 Hz, 2H, $2H_m$), 6.99 (br. s, 1H, P_4), 3.83 (s, 3H, CH_3O), 2.02 (s, 3H, CH_3). HRMS(ES): m/z 1715.64 ($[M - PF_6]^+$; calcd, 1715.15), 785.59 ($[M - 2PF_6]^{2+}$; calcd, 786.09), 475.16 ($[M - 3PF_6]^{3+}$; calcd, 475.74), 320.12 ($[M - 4PF_6]^{4+}$; calcd, 320,82). TLC, R_f = 0.25 in acetone/H_2O/aq. KNO_3 = 9:1:0.5.

[Ru(bpy)$_2$(PT)Os(tpy)][PF$_6$]$_4$ (RPTO). A solution of **RPT** (0.37 g, 0.30 mmol) and $[Os(tpy)Cl_3]$ (0.16 g, 0.30 mmol) in ethylene glycol (8 mL) was heated under Ar at 200 °C overnight. The mixture was allowed to reach room temperature, and aqueous KPF_6 (50 mL) was added. The resulting precipitate was filtered and purified by column chromatography (silica gel, CH_2Cl_2/MeOH gradient elution from 98:2 to 80:20) to afford **RPTO** (0.26 g, 40%) as a red-brown solid. ^{1}H NMR (CD_3CN, 300 MHz): δ 8.79−8.65 (m, 5H, P_7, $2t_{3'}$, 2T), 8,55−8.38 (m, 8H, P_2, $4b_3$, $2t_3$, $T_{3''}$), 8.34 (d, J=8.4 Hz, 1H, 1T), 8.25 (d, J=9.0 Hz, 1H, P_5/P_6), 8.14 (d, J = 9.0 Hz, 1H, P_5/P_6), 8.15−7.75 (m, 12H, P_9, $4b_4$, $1b_6$, $2t_4$, $t_{4'}$, $T_{4''}$, 2T), 7.67(d, J=5.4 Hz, 1H, b_6), 7.62 (br. d, J = 8.4 Hz, 1H, 1T), 7.55−7.50 (m, 2H, $2b_6$), 7.48 (d, J = 8.9 Hz, 2H, $2H_o$), 7.46−7.41 (m, $2b_5$), 7.25−7.18 (m, 5H, $2b_5$, $2t_6$, $T_{6''}$), 7.10−7.05 (m, 2H, $2t_5$), 7.02 (d, J=8.9 Hz, 2H, $2H_m$), 6.86 (s, 1H, P_4), 3.83 (s, 3H, CH_3O), 2.05 (s, 3H, CH_3). HRMS-(ES): m/z 1804.7 ($[M - PF_6]^+$; calcd, 1805.2), 830.7 ($[M - 2PF_6]^{2+}$; calcd, 831.1), 504.9 ($[M - 3PF_6]^{3+}$; calcd, 505.4). TLC, R_f = 0.25 in MeCN/H_2O/aq. KNO_3 = 9:1:0.3.

Physical Measurements. ^{1}H NMR spectra were recorded on a Bruker DPX300 (300 MHz) or a Bruker AV400 (400 MHz) NMR spectrometer. All measurements were carried out in CD_3CN, using the residual solvent peak as the internal reference. ES-mass spectra were obtained with a Waters Micromass ZQ spectrometer in the positive ion mode. The extraction cone voltage was set to 10 V to avoid fragmentations. In all of the cases, a well-resolved isotopic pattern consisting of monoisotopic peaks separated by $1/z$ Da was obtained. Optically dilute solutions were used thorough all of the photophysical measurements. UV/vis absorption spectra were recorded on a JASCO 570 UV/vis−NIR or a JASCO 630 UV/vis spectrophotometer with 1-cm-path-length quartz cells. Absorption maxima are ±2 nm; molar absorption coefficients are ±10%. Emission spectra were recorded using a JASCO-7200 spectrofluorimeter equipped with a red-sensitive Hamamatsu R928 detector. Luminescence quantum yields of the complexes were measured according to literature procedures using $[Ru(bpy)_3]Cl_2$ as the standard;[28] estimated uncertainties are ±15% or better. For ligand **PT**, the quantum yield was measured using the "absolute PL quantum yield measurement system" from Hamamatsu, model C9920−02. Emission lifetime measurements were carried out using time correlated single photon counting (Edinburgh Analytical Instruments) in a T setting, consisting of an nF900 (N_2 filled) flashlamp, J-yA monochromators, and a single photon photomultiplier detection system, model S 300 detector, with a Norland N5000 MCA card. The F900 Program (version 5.13) is used for data processes, with the quality of fits determined by examination of the χ^2 and residual plots of the fitted functions. Lifetimes were recorded in acetonitrile deaerated by continuous N_2 bubbling and are ±10 ns. Cyclic voltammetry and differential pulse experiments were performed on an Autolab PGSTAT12 potentiostat/galvanostat instrument at room temperature, under nitrogen, in a single compartment electrochemical cell. A three-electrode configuration was used containing 0.1 M tetrabutylammonium hexafluorophosphate as the supporting electrolyte (electrochemical grade) and anhydrous acetonitrile as the solvent. As a reference, a 0.1 M $AgNO_3$ CH_3CN Ag/Ag^+ electrode was used. The counterelectrode was a platinum wire, and as a working electrode, platinum or glassy carbon Ø 2 mm electrodes were used. All solutions were degassed thoroughly for at least 15 min with argon, and an inert gas blanket was maintained over the solution during the measurements. Analyte concentrations of typically 1 mM were used.

Titration Experiments. For the titration experiments, the absorption and luminescence spectra of a 10^{-5} M solution of the Ru(II) complex **RPT** in CH_3CN/H_2O (1:1) were recorded. Then, aliquots (1×10^{-6} to 1×10^{-3} M) of aqueous $ZnCl_2$, $Cu(NO_3)_2$, $Mg(SO_4)$, $NiCl_2$, $FeSO_4$, $CoCl_2$, $CrCl_2$, and $AgNO_3$ solutions or trifluoroacetic acid were added, and the absorbance and fluorescence spectra were recorded again. The change in the total volume of the solution was kept below 10% in all of the experiments.

Results and Discussion

Synthesis. The synthesis of the target dinuclear Ru(II)/Os(II) metal complexes **RPTR** and **RPTO** was first attempted starting from the multitopic bridging ligand **PT** by stepwise metal complexation of its phen and tpy binding units. However, reaction of **PT** with either *cis*-$[Ru(bpy)_2Cl_2]$ or $[Ru(tpy)Cl_3]$ to obtain a mononuclear Ru complex led in all cases to mixtures of different metal complexes, which were difficult to separate.

To avoid these problems, we decided to follow a "building block" approach for the synthesis of the bimetallic assemblies.[19,23,29,30] Thus, the key bromo-substituted tris-bidentate ruthenium complex **RP** (Scheme 1) was prepared by reacting bromophenanthroline **1** with *cis*-$[Ru(bpy)_2Cl_2]\cdot 2H_2O$ in ethylene glycol at 150 °C overnight. The boronate ester tpy derivative **2** was obtained from the reaction of 5-bromo-5″-methyl-2,2′:6′,2″-terpyridine with bis(neopentyl glycolato)diboron in the presence of a catalytic amount of $PdCl_2$(dppf).[24,25] The mononuclear Ru(II) complex **RP** was then cross-coupled with ligand **2** under standard Suzuki coupling conditions (Pd(0), Na_2CO_3 as the base, DMF/water as solvent).[31] In this case, **RPT** was isolated in 50% yield after ion exchange with aqueous KPF_6 and purification through a silica column. In a second metalation step, this complex was reacted with $[M(tpy)Cl_3]$ (M = Ru(II) or Os(II)) in ethylene glycol at 150 or 200 °C overnight, followed by anion exchange with aqueous KPF_6 and purification by column chromatography, to yield the pure dinuclear compounds **RPTR** and **RPTO** with 47% and 40% yield, respectively (Scheme 1). All of the complexes were characterized by ^{1}H NMR spectroscopy and ES-MS. The proton chemical shifts were assigned with the aid of standard COSY experiments and by comparison with those of similar compounds.[21,25]

Encouraged by the successful modular approach for the synthesis of the mononuclear Ru−phen complex **RPT**, we decided to attempt the synthesis of the equivalent mononuclear Ru−tpy complex **PTR**, starting from appropriate bis-terdentate ruthenium complex precursors. Thus, we synthesized a bromo-substituted $Ru(tpy)_2$ complex (**RT**) from 5-bromo-5″-methylterpyridine[25] and

(28) Eaton, D. F. *Pure Appl. Chem.* **1988**, *60*, 1107–1114.

(29) Cassidy, L.; Horn, S.; Cleary, L.; Halpin, Y.; Browne, W. R.; Vos, J. G. *Dalton Trans.* **2009**, 3923–3928.

(30) Halpin, Y.; Cleary, L.; Cassidy, L.; Horne, S.; Dini, D.; Browne, W. R.; Vos, J. G. *Dalton Trans.* **2009**, 4146–4153.

(31) Barigelletti, F.; Flamigni, L.; Balzani, V.; Collin, J.-P.; Sauvage, J.-P.; Sour, A.; Constable, E. C.; Thompson, A. M. W. C. *J. Am. Chem. Soc.* **1994**, *116*, 7692–7699.

Scheme 1. Synthetic Scheme for Preparation of the Mononuclear and Dinuclear Metal Complexes[a]

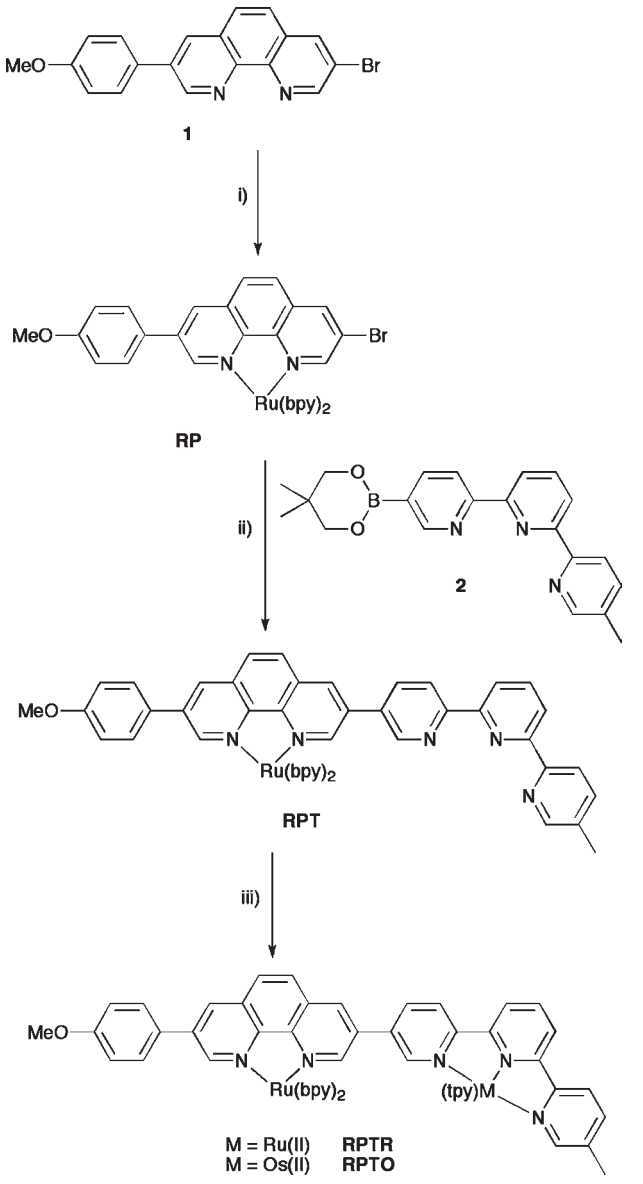

[a] (i) $[Ru(bpy)_2Cl_2]$ ethylene glycol 150 °C, 90%. (ii) $[Pd(PPh_3)_4]$, K_2CO_3, DMF/H_2O 150 °C, 50%. (iii) **RPTR:** $[Ru(tpy)Cl_3]$ ethylene glycol 150 °C, 47%. **RPTO:** $[Os(tpy)Cl_3]$ ethylene glycol, 200 °C, 40%.

$[Ru(tpy)Cl_3]$. However, we failed to obtain the corresponding boronic ester derivative of the phen ligand **1**,[24] as well as to transform **RT** into a boronic ester derivative for Suzuki coupling. In all attempts, mainly starting materials and different amounts of the corresponding protiodehalogenated derivatives were recovered. Consequently, we decided to abandon this route.

Spectroscopic properties. The UV−vis absorption spectra of ligand **PT** in deoxygenated $CHCl_3$ and complexes **RP**, **RPT**, **RPTR**, and **RPTO** in deoxygenated acetonitrile at room temperature are shown in Figure 1. **PT** exhibits two absorption maxima in the UV region, at 283 and 341 nm. In the metal complexes, as observed for other ruthenium and osmium polypyridyl complexes and by comparison with the spectrum of **PT**, peaks and shoulders between 200 and 400 nm are assigned to ligand-centered transitions.[2,3,24,25]

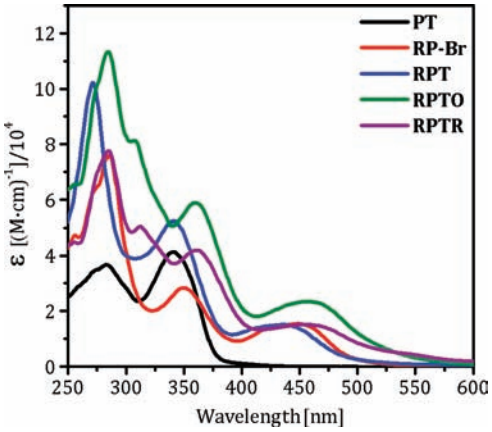

Figure 1. UV/vis absorption spectra of **PT** (deoxygenated $CHCl_3$) and **RP**, **RPT**, **RPTO**, and **RPTR** (deoxygenated acetonitrile) at room temperature.

A broad absorption centered around 450 nm, is assigned to a metal-to-ligand charge-transfer (MLCT) transition (Table 1) as observed in related ruthenium and osmium oligopyridine complexes.[1−4] On going from **RP** and **RPT** to the dinuclear complexes **RPTR** and **RPTO**, the MLCT band is slightly red-shifted. In **RPTO**, there is also a low-intensity tail extending up to 760 nm, not shown in Figure 3, that can be assigned to the spin-forbidden MLCT transitions associated with the Os−tpy unit.[32]

Luminescence spectra (Figure 2) at room temperature were obtained in deoxygenated acetonitrile. In the experiments, the excitation wavelength was varied according to the absorption properties of the complexes. By comparison with other polypyridine ruthenium(II) complexes,[1−4] this luminescence was assigned to emission from the ^{3}MLCT state.

For the mononuclear compounds **RP** and **RPT**, emission maxima (λ_{em}), quantum yields (Φ), and lifetimes (τ) are well described by a monoexponential fit. They are similar to those previously reported in other mononuclear tris-bidentate ruthenium complexes formed from bpy and phen ligands. In the case of the dinuclear **RPTO** complex, we recorded emission spectra at two different excitation wavelengths: 454 and 525 nm. At 525 nm, the difference between molar absorption coefficients of **RPT** and **RPTO** is maximized (Figure 1), and the absorption is mainly due to the Os−tpy chromophore. On the other hand, absorption at 454 nm is due to the superposition of both Ru−bpy and Os−tpy chromophores. The excitation of **RPTO** into the peak at 525 nm resulted in the appearance of a luminescence band centered around 756 nm ($\Phi = 0.0071$), which is reminiscent of that found for the related $[Os(tpy)_2]^{2+}$ mononuclear complex. However, when we excited the band at 454 nm, we observed two bands centered around 636 and 756 nm. The new band at 636 nm was assigned to emission from the Ru−bpy unit in **RPTO**. The lower emission intensity at 636 nm in **RPTO** compared with that of **RPT** (Table 1 and Figure 2) suggests an efficient energy transfer from Ru−bpy to the Os−tpy center occurring with ca. 95% quenching of the emission from the Ru−bpy chromophore. The big separation between

(32) Kumaresan, D.; Shankar, K.; Vaidya, S.; Schmehl, R. *Top. Curr. Chem.* **2007**, *281*, 101–142.

Table 1. Photophysical Properties for **PT** and the Metal Complexes[a]

compound	$\lambda_{MLCTmax}$[nm]	ε [$M^{-1}\cdot cm^{-1}$]	λ_{em} [nm][b]	Φ[b]	τ [ns][c]	ref
PT			405	1		
$[Ru(bpy)_3]^{2+}$	450	11 900	613	0.059[33]	1004	
$[Ru(tpy)_2]^{2+}$	474	14 600	629	$\leq 5 \times 10^{-6}$	0.25[d]	33, 34a
$[Os(tpy)_2]^{2+}$	475/656	15 400/4200	729	0.014[d]	269	33, 34b
RP	451	15 500	618	0.059	1300	
RPT	435	15 100	624	0.062	1580	
RPTO	454	15 200	636/756		132/88	
RPTR	458	23 400	634	0.0014	< 10	

[a] $[Ru(bpy)_3]^{2+}$, $[Ru(tpy)_2]^{2+}$, and $[Os(tpy)_2]^{2+}$ data have been added for comparison. Measured at room temperature in deoxygenated acetonitrile, except for **PT** (deoxygenated $CHCl_3$). [b] $\lambda_{ex} = \lambda_{MLCTmax}$ except for **PT** $\lambda_{ex} = 341$ nm. [c] $\lambda_{ex} = 337$ nm. [d] In deaerated EtOH/MeOH.

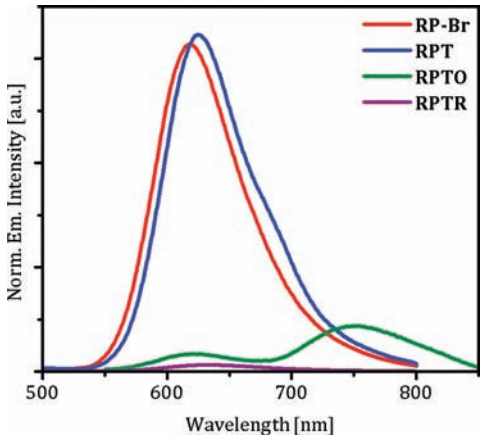

Figure 2. Luminescence spectra ($\lambda_{ex} = \lambda_{MLCTmax}$) of complexes **RP**, **RPT**, **RPTO**, and **RPTR** in deoxygenated acetonitrile at room temperature. The areas under the curves have been scaled according to Φ of the emission. In the case of RPTO, both emissions have been considered for the scaling.

Ru−bpy and Os−tpy emissions makes the calculation of both emission lifetimes possible. The lifetime of the Ru-based emission (τ_{RPTO} = 132 ns) is notably shorter than that recorded for **RPT** (τ_{RPT} = 1580 ns) under the same conditions. This supports the suggestion that emission from the Ru−bpy moiety in **RPTO** is quenched by intramolecular energy transfer. The rate constant for triplet energy transfer, $k_{TT} = 6.9 \times 10^6$ s^{-1}, was determined as the difference between the inverse of the two triplet lifetimes for the Ru−tpy emission:

$$k_{TT} = \tau_{RPT}{}^{-1} - \tau_{RPTO}{}^{-1}$$

For the **RPTR** complex, a single emission centered at 634 nm with a low quantum yield (Φ = 0.0014) and short lifetime < 10 ns was detected. These data suggest a Ru−tpy-centered emission, and this indicates that the quenching of the Ru−bpy moiety is complete. That is most likely caused by an energy transfer process from the normally highly emissive, long-lived Ru−bpy unit toward the short-lived Ru−tpy chromophore.

Electrochemistry. The electrochemical properties of the complexes synthesized were studied using cyclic voltammetry (CV) and differential pulse voltammetry (DPV). All oxidation and most of the reduction processes observed are quasi-reversible and are presented in Table 2, along with values obtained for appropriate model systems. An example of the electrochemical response is illustrated in Figure 3 for the mononuclear **RPT** and the dinuclear **RPTO** complexes.

For the **RP** and **RPT** mononuclear complexes, a single cathodic process at ca. 1.30 V is observed that can be assigned, by comparison with the model compounds, to a Ru-based monoelectronic oxidation. For the dinuclear **RPTR** complex, a single two-electron oxidation peak is observed at 1.31 V, indicating that both ruthenium centers are oxidized at the same potential. In the case of the heterometallic **RPTO** complex, two single-electron peaks, ascribed to the successive Os^{II}/Os^{III} and Ru^{II}/Ru^{III} oxidations, are observed at 0.96 and 1.33 V, respectively. The fact that oxidation in the dinuclear compounds occurred with no significant shift of the peaks, compared to that of the parent mononuclear complexes, suggests the absence of significant electronic coupling between both metal centers in the ground state.

For all compounds, only three reduction peaks are clearly observed. The first two peaks correspond to quasi-reversible one-electron processes. For **RP** and **RPT** also, the third reduction peak is quasi-reversible. However, in **RPTR** and **RPTO** complexes, the third reduction peaks, centered around −1.5 V, appear in the CV and DPV as sharp peaks, which are most likely due to the adsorption of the highly reduced complexes on the electrode.[37]

Generally, modification of an oligopyridine ligand by a pyridine substituent, e.g., when going from $[Ru(tpy)_2]^{2+}$ to $[Ru(tpy\text{-}py)_2]^{2+}$ (tpy-py = 4′-(4-pyridyl)-tpy), results in a shift of the ligand reduction potential to a less negative potential.[21] This trend is clearly observed on going from **RP** (−1.35 V) to **RPT** (−1.21 V), in which a pendant free tpy unit is present and suggests that the first reduction in **RPT** is centered on the **PT** ligand. In the case of **RPTR** and **RPTO**, as a result of the capping of the free tpy unit in **RPT** with Ru(II) and Os(II) metallo-fragments, the reduction potential was further displaced toward less negative potentials (from ca. −1.2 to −1.0 V). These observations suggest that the LUMO orbital of the dinuclear complex is located on the bridging ligand and that considerable delocalization of the LUMO over the tpy and bpy moieties of the bridging ligand is taking place. A similar observation is made for the related ruthenium and osmium complexes containing the bis(bpy) type bridging

(33) Montaldi, M.; Credi, A.; Prodi, L.; Gandolfi, M. T. *Handbook of Photochemistry*, 3rd ed.; Taylor and Francis: New York, 2006.
(34) (a) Maestri, M.; Armaroli, N.; Balzani, V.; Constable, E. C.; Thompson, A. M. W. C. *Inorg. Chem.* **1995**, *34*, 2759–2767. (b) Constable, E. C.; Thompson, A. M. W. C. *J. Chem. Soc., Dalton Trans.* **1994**, 1409–1418.
(35) Harriman, A.; Mayeux, A.; Stroh, C.; Ziessel, R. *Dalton Trans.* **2005**, 2925–2932.
(36) Caspar, J. V.; Meyer, T. J. *Inorg. Chem.* **1983**, *22*, 2444–2453.
(37) Bard, A. J.; Foster, L. R. *Electrochemical Methods, Fundamentals and Applications*, 2nd ed.; John Wiley and Sons: New York, 2001.

Table 2. Oxidation and Reduction Formal Potentials[a] for **RP**, **RPT**, **RPTR**, and **RPTO** Obtained from DPV Experiments

compound	$Ru^{II}-Ru^{III}$	$Os^{II}-Os^{III}$	reduction potentials			ref
$[Ru(bpy)_3]^{2+}$	1.29		−1.30	−1.54	−1.75	35
$[Ru(tpy)_2]^{2+}$	1.30		−1.24	−1.49		35
$[Ru(bpy)_2(phen)]^{2+}$	1.29		−1.36			36
$[Os(tpy)_2]^{2+}$		0.97	−1.23	−1.52		31
RP	1.31(81)		−1.35(60)	−1.56(111)	−1.77(70)	
RPT	1.30(90)		−1.21(61)	−1.34(150)	−1.70	
RPTR	1.31(90)		−1.03(71)	−1.20(60)	−1.48(s)	
RPTO	1.33(71)	0.96(71)	−1.00(70)	−1.18(81)	−1.45(s)	

[a] Recorded in CH_3CN containing 0.1 M NBu_4PF_6; $E_{1/2}$ in V vs SCE. The values in parentheses are the differences between the anodic and cathodic peaks of the CV waves (mV), (s) = spiked-shaped peak.

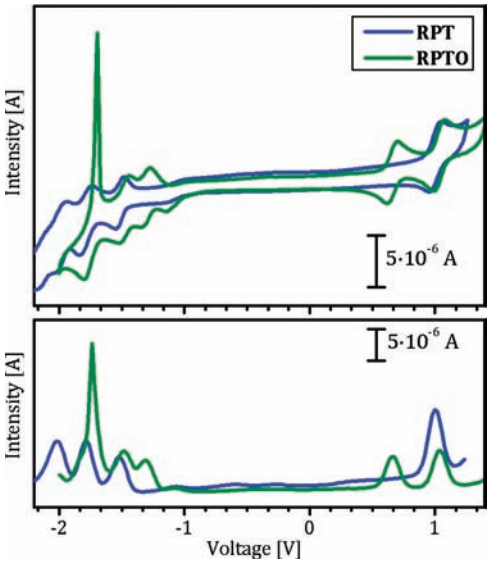

Figure 3. CV and DPV vs SCE in deoxygenated acetonitrile for **RPT** and **RPTO** at 100 mV/s.

ligand.[28] So the electrochemical data show that while coordination of the bridging ligand produces a lowering of the LUMO, the HOMO (represented by the first oxidation) is insensitive to the coordination of the second metal.

Luminescent Sensing of Complex RPT with Respect to Transition Metal Cations. The electronic properties of polypyridyl Ru(II) complexes covalently linked to appropriate free binding units can vary upon coordination of a metal ion. These changes have been applied in the development of luminescent sensors.[5,6] For the complex **RPT**, the free tpy coordinating site connected to a tris-bidentate Ru(II) unit may act as a potential binding site for transition metal ions. This capability was explored by titrating acetonitrile−water (1:1 v/v) solutions containing **RPT** with different metal salts and also with trifluoroacetic acid (TFA), while monitoring the absorption and emission intensities. In all cases, the absorption spectrum remains basically unaltered while changes are observed in the emission spectrum. Thus, while the addition of Mg(II) and Ag(I) diamagnetic metals or TFA does not affect the emission properties, the emission intensity sharply decreases when paramagnetic Cu(II), Co(II), Fe(II), and Ni(II) metals are added. Finally, a clear increase in intensity and a red shift of the $\lambda_{MLCTmax}$ of the emission is observed when Zn(II) is introduced in the solution.

The decrease in the emission intensities can be accounted by the heavy atom effect and the paramagnetic nature of the metal centers,[33] most likely because of

Table 3. Luminescence Properties for **RPT** and **RPT−Zn** Complexes in CH_3CN and $CH_3CN:H_2O$ (1:1 v/v)

		CH_3CN		CH_3CN/H_2O	
complex	λ_{em}[a] [nm]	Φ	τ [ns]	Φ*	τ [ns]
RPT	624	0.062	1580	0.050	294
RPT−Zn[b]	638	0.083	2096	0.056	430

[a] λ_{ex} = 435 nm. [b] 10 equivalents of Zn (ZnOTf in CH_3CN or $ZnCl_2$ in water) were added to the solution.

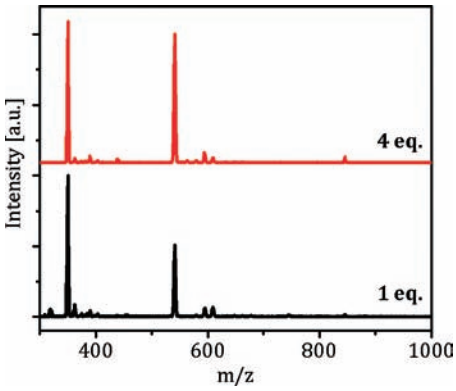

Figure 4. MS(ES) of a solution of **RPT** (1×10^{-5} M) in CH_3CN/H_2O (1:1 v/v) with different amounts of $ZnCl_2$.

electron transfer from the triplet excited state of the ruthenium moiety, while the increase upon addition of Zn(II) can be attributed to an increase in the delocalization of the electronic density over the **PT** bridge in the **RPT−Zn** complex and potentially to an increased rigidity of the molecular system upon coordination. Others have already reported similar effects.[19,35,38,39] This delocalization results in the stabilization of the lowest energy Ru−PT ^{3}MLCT state in **RPT−Zn** complex when compared with **RPT**, in a bathochromic shift of the emission, in an increase in the quantum yield, and in a longer lifetime (Table 3).

Electrospray mass spectra of CH_3CN-H_2O solutions of **RPT** containing 1 equiv and 4 equiv of $ZnCl_2$ (Figure 4) only revealed the presence of the **RPT−Zn** complex with 1:1 stoichiometry (m/z 350 $[Zn(\mathbf{RPT})Cl]^{3+}$ and 542 $[Zn(\mathbf{RPT})Cl_2]^{2+}$). In view of Zn−tpy association constants of the 1:1 and 1:2 complexes,[40] the lack of peaks corresponding to $Zn(\mathbf{RPT})_2$ complexes could reflect an increased

(38) Barigelletti, F.; Flamigni, L.; Calogero, G.; Hammarström, L.; Sauvage, J.-P.; Collin, J.-P. *Chem. Commun.* **1998**, 2333–2334.
(39) Hu, Y. Z.; Xiang, Q.; Thummel, R. P. *Inorg. Chem.* **2002**, *41*, 3423–3428.
(40) Benniston, A. C.; Harriman, A.; Lawrie, D. J.; Mayeux, A.; Rafferty, K.; Russell, O. D. *Dalton Trans.* **2003**, 4762–4769.

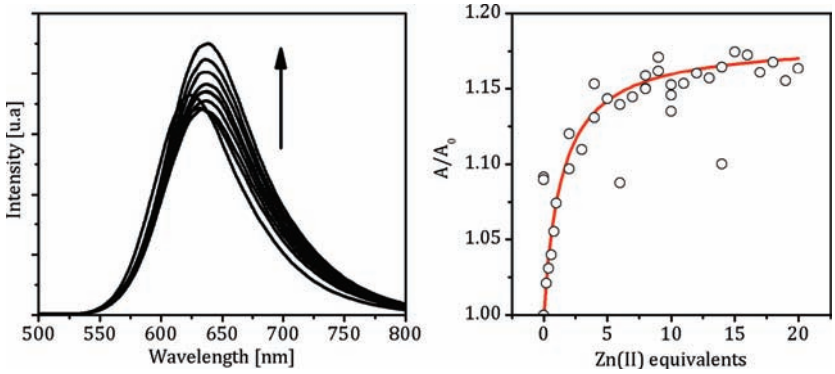

Figure 5. Titration of a solution of **RPT** (1×10^{-5} M) in CH_3CN/H_2O with different amounts of $ZnCl_2$. Changes in the emission spectra (left) and evolution of the area under the emission curve (right) as a function of the Zn(II) equivalents added: (○) experimental, (—) fitted according to eq 1.

steric hindrance around the tpy coordinating unit in **RPT**, due to the presence of the bulky Ru−bpy center.

To determine the binding constant for the formation of the 1:1 complex, we monitored the evolution in the luminescence of a solution of **RPT** upon the addition of different amounts of $ZnCl_2$. These luminescence changes (Figure 5) were analyzed according to eq 1 where C_{Zn} is the total Zn(II) concentration in solution and A and A_0 are the areas under the emission curve in the presence and in the absence of Zn(II). A_∞ is the area at infinite Zn(II) concentration, and K is the binding constant for the formation of a 1:1 complex.[39]

$$\frac{A}{A_0} = \frac{1 + \left(\frac{A_\infty}{A_0}\right) \cdot K \cdot C_{zn}}{1 + K \cdot C_{zn}} \qquad (1)$$

For **RPT**, this binding constant was estimated to be $1.5 \times 10^5\ M^{-1}$; this value is in the range of what is expected for a $[Zn(tpy)]^{2+}$ complex.[40]

Conclusions

In this study, we have successfully used cross-coupling Suzuki methodologies in a "building block" approach for the synthesis of the **RPT** complex. The free tpy unit in **RPT** was further capped with suitable metallo fragments to yield a series of new Ru, Os, and Zn dinuclear complexes: **RPTR**, **RPTO**, and **RPT−Zn**. In this way, we have increased the so far rather limited number of dinuclear compounds where metals are connected through heteroditopic oligopyridine ligands. In our case, metals are connected through a bridge incorporating phen and tpy units directly connected to one another. We have fully characterized the new complexes and studied their spectroscopic and electrochemical properties. We have shown that the metal centers bridged by the **PT** ligand in the dinuclear complexes do not interact with each other in the ground state and that the LUMO orbital of the dinuclear complex is located on the bridging ligand. For **RPTR**, the two ruthenium centers are of comparable energy, both in terms of redox chemistry and excitation energies. The emission lifetime data suggest that the lowest-energy triplet excited state is based on the tpy moiety and that energy transfer from the phen to the tpy unit is effective. The dinuclear complex **RPTO** also displays intramolecular triplet energy transfer. However, for this compound the process is considerably slower, and as a result, a dual emission is observed while the lowest-energy triplet is clearly localized on the Os(tpy) unit. Analysis of the luminescent properties indicates that in the **RPT-Zn** complex the triplet state is of MLCT character but is more extensively delocalized than in **RPT**. At present, detailed temperature-dependent emission measurements are being undertaken to further investigate these intercomponent interaction processes.

Acknowledgment. We thank the Spanish Ministerio de Ciencia e Innovación, with FEDER cofinancing, for financial support (projects MAT2007-61584 and CSD 2007-00010, Consolider-Ingenio in Molecular Nanoscience) and the Generalitat Valenciana (Project PROMETEO/2008/128, Project PROMETEO/2009/095 and GVPRE/2008/152). S.T. thanks the MEC for a predoctoral fellowship. J.G.V. thanks Science Foundation Ireland for financial support under Grant No. 07/SRC/B1160 Advanced Biomimetic Materials for Solar Energy Conversion.